Monitoring of hexyl 5-aminolevulinate-induced photodynamic therapy in rat bladder cancer by optical spectroscopy

Eivind L. P. Larsen
Lise L. Randeberg
Norwegian University of Science and Technology
Department of Electronics and Telecommunications
N-7034 Trondheim, Norway

Odrun A. Gederaas
Norwegian University of Science and Technology
Department of Cancer Research and Molecular
    Medicine
N-7006 Trondheim, Norway

Carl-Jørgen Arum
Norwegian University of Science and Technology
Department of Cancer Research and Molecular
    Medicine
N-7006 Trondheim, Norway
    and
St. Olavs Hospital
Trondheim University Hospital
Department of Surgery
N-7006 Trondheim, Norway

Astrid Hjelde
Norwegian University of Science and Technology
Department of Circulation and Medical Imaging
N-7006 Trondheim, Norway

Chun-Mei Zhao
Duan Chen
Hans E. Krokan
Norwegian University of Science and Technology
Department of Cancer Research and Molecular
    Medicine
N-7006 Trondheim, Norway

Lars O. Svaasand
Norwegian University of Science and Technology
Department of Electronics and Telecommunications
N-7034 Trondheim, Norway

Abstract. Monitoring of the tissue response to photodynamic therapy (PDT) can provide important information to help optimize treatment variables such as drug and light dose, and possibly predict treatment outcome. A urinary bladder cancer cell line (AY-27) was used to induce orthotopic transitional cell carcinomas (TCC) in female Fischer rats, and hexyl 5-aminolevulinate (HAL, 8 mM, 1 h)-induced PDT was performed on day 14 after instillation of the cancer cells (20 J/cm^2 fluence at 635 nm). *In vivo* optical reflectance and fluorescence spectra were recorded from bladders before and after laser treatment with a fiberoptic probe. Calculated fluorescence bleaching and oxygen saturation in the bladder wall were examined and correlated to histology results. Reflectance spectra were analyzed using a three-layer optical photon transport model. Animals with TCC treated with PDT showed a clear treatment response; decreased tissue oxygenation and protoporphyrin IX (PpIX) fluorescence photobleaching were observed. Histology demonstrated that 3 of 6 animals with treatment had no sign of the tumor 7 days after PDT treatment. The other 3 animals had significantly reduced the tumor size. The most treatment-responsive animals had the highest PpIX fluorescence prior to light irradiation. Thus, optical spectroscopy can provide useful information for PDT. The model has proved to be very suitable for bladder cancer studies. © *2008 Society of Photo-Optical Instrumentation Engineers.*
  [DOI: 10.1117/1.2967909]

1 Introduction

Urinary bladder cancer causes more than 130,000 deaths every year worldwide.[1] The strongest known risk factor for bladder cancer is smoking, probably due to the high content of carcinogenic arylamines in cigarette smoke. The bladder consists of three layers: a mucous layer of epithelial cells (urothelium), the underlying submucosa, and the outer muscular layer. Bladder cancer usually originates in the epithelial lining and can continue to grow through the submucosa into the muscular layer, then invade surrounding tissues and the lymph vessels, giving rise to metastasis. Treatment of bladder cancer depends on the stage of the disease, the type of cancer, and the patient's age and general health condition. Treatment options include surgery, endoscopic resection, chemotherapy, and immunotherapy.

Photodynamic therapy (PDT) is a treatment modality that has been shown to be effective for both malignant and non-

Address all correspondence to: Eivind L.P. Larsen, Norwegian University of Science and Technology, Department of Electronics and Telecommunications, N-7491 Trondheim, Norway; Tel: +4773592776; Fax: +4773591441; E-mail: eivind.larsen@iet.ntnu.no.

malignant diseases.[2] PDT is based on photochemical reactions between a photosensitizer and light, where the sensitizer accumulates in the tissue and is activated by light of an appropriate wavelength. This in turn induces cell death in the tissue by the production of singlet oxygen and other reactive oxygen species (ROS).[3] Since cancer cells have a higher accumulation of sensitizer than normal cells,[4] PDT is a selective treatment modality. To achieve curative treatment with PDT, it is crucial to find the right balance between the drug doses and light doses to destroy cancerous tissue and avoid irreparable damage to surrounding tissues.

A number of photosensitizers are currently available, among which 5-aminolevulinic acid (ALA) is a well-studied drug for PDT. ALA is not a photosensitizer in itself, but it is a precursor to the photosensitizer protoporphyrin IX (PpIX) via the heme-biosynthesis. When ALA is taken up by cells, it is endogenously converted into PpIX.[5] New ALA derivatives such as hexyl 5-aminolevulinate (HAL) may increase the efficiency of PDT due to the high lipophilicity of the ALA esters compared to ALA, leading to better penetration into the cells and ultimately a higher concentration of PpIX.[6–8]

Optical spectroscopy (e.g., fluorescence, reflectance, near-infrared, and Raman spectroscopy) is commonly used for diagnostics in medicine and can provide important information on the tissues studied. PpIX fluorescence has been used to aid white-light cystoscopy for the detection and diagnosis of bladder cancer, because the fluorescence demarcates the area of carcinomas *in situ*, enhancing the detection sensitivity.[9–12] PpIX exhibits a characteristic dual-peaked fluorescence, with a main emission peak around 635 nm and a second emission peak around 705 nm.[13,14]

Molecular oxygen is crucial for the sensitivity of tumor cells to PDT and is consumed during irradiation. Since the cytotoxic effects depend on oxygen, monitoring tissue oxygenation before and after PDT may predict the effect of the treatment.[15]

The value of optical measurements depends strongly on the method of analysis chosen. Empirically based formulas that use a set of wavelengths is the most common method to evaluate reflectance spectra. In most cases this approach is sufficiently accurate. However, in complex systems involving several chromophores, such a method may cause problems. A photon transport model can be used to identify the various constituents present in the measured spectra by, e.g., simulating spectra with a given chromophore combination and comparing them iteratively to the measurements.

Superficial urinary bladder cancer is suited for effective treatment by PDT because the bladder is easily accessible for both intravesical instillation and illumination. Intravesical instillation has been shown to cause less damage to normal tissue than intravenous instillation and still yields the same PDT efficacy.[16] Current limitations to ALA-based PDT is the penetration depth in tissues of both the sensitizer and the illumination used in intravesical treatment. This limited penetration depth suggests that PDT may be most effective on low-stage (superficial) cancers.[17]

The aim of the present study was to investigate whether *in vivo* reflectance and fluorescence spectroscopy are useful methods in predicting the therapeutic efficacy of PDT, using HAL in a superficial urinary bladder cancer model.

2 Modeling

2.1 Bladder Geometry and Light Fluence

The thickness of the rat bladder wall varies between 0.1 and 1.0 mm, depending on the absence or presence of a tumor. The relative thickness of the muscular layer compared to urothelium and submucosa is related to the degree of tumor infiltration. For the calculation of light fluence, the rat bladder is modeled as a sphere with a volume of 0.3 ml, corresponding to an internal bladder surface area of 2.2 cm^2.

During illumination, the light is multiply reflected inside the bladder, which causes a locally higher effective irradiance. This behavior is known as the integrating sphere effect, and might cause a significantly higher light dose than the intended dose without compensation it. The increased irradiance depends on the optical characteristics (reflection factor ρ) of the bladder tissue; however, there can be large variations of this parameter between different bladders.[18]

The total fluence rate ϕ inside the bladder is the sum of the input light and the multiple reflected light:[18]

$$\phi(r) = P\left(\frac{1}{4\pi r^2} + \frac{\beta - 1}{4\pi R^2}\right), \qquad (1)$$

where r is the radial distance to the diffuser, R is the actual radius of the bladder cavity, P is the laser power, and β is the ratio between the total light fluence and the nonscattered light fluence rate, which is approximated to $1/(1-\rho)$.

Light is necessary for the photochemical processes to produce ROS and cause cell damage. However, cell damage may also be caused by factors other than the ROS. Thermal damage or heat-induced necrosis (burns) can also contribute to the resulting cell damage after illumination. Thus, the temperature increase in the bladder during the illumination process must be considered. The temperature will typically reach a steady-state value after 5 minutes of exposure. To avoid thermal damage (and pain), the temperature should not exceed 45 °C.[19] It is therefore necessary to evaluate the temperature increase in the bladder during the illumination process. The steady-state temperature distribution can be found from the bioheat equation.[20]

Worst-case calculations (all light absorbed, no blood perfusion) for the fluence rate used in this experiment give a less than 3 °C temperature increase, which does not exceed a tolerable level.

2.2 Simulations

A mathematical model was used to simulate the measured spectra in order to extrude more information. The model is an analytical photon transport model based on the diffusion approximation[21] and adapted to fit bladder parameters. The model consists of two flat layers to represent the urothelium and submucosa on top of a semi-infinite slab that represents the muscular layer and underlying tissue. Data for the optical properties of the bladder were found in the literature.[22,23] The boundary between the water and the urothelium was represented by refraction indices $n_{water}=1.33$ and $n_{urothelium}=1.36$, and the anisotropy factor g for the tissue scattering was set to $g=0.93$ at 630 nm. The blood hematocrit for rats was set to 47%.[24]

Due to the short penetration length of light below 700 nm, most of the reflected light was from the bladder layers. With the dimensions kept fixed, the blood volume (BV) fraction and the oxy-, deoxy,- and methemoglobin content in the model were iterated to yield the best fit with the measured spectrum. The bladder dimensions used for analysis were 75 μm for the urothelium and submucosa, and 300 μm for the muscle layer.

3 Materials and Methods

The efficacy of HAL-induced PDT was studied in an animal bladder cancer model in which a superficial rat bladder cancer cell line (AY-27) was instilled in rat bladders. Whole-bladder-wall PDT was performed on these rats after HAL was administered intravesically. The treatment was performed on day 14 after initial instillation of the transitional cell carcinoma cells, and histology was performed on day 21. All animal experiments were approved by the national animal research authority.

3.1 Chemicals

RPMI-1640 medium, L-glutamine, fetal calf serum (FCS), fungizone, penicillin-streptomycine, trypsin, and phosphate buffered saline (PBS) were obtained from Gibco BRL, Life Technologies (Inchinnan, Scotland). Gentamicin sulphate was obtained from Schering Corp (Kenilworth, NJ), and HAL was supplied by Photocure ASA (Oslo, Norway). Ultra-purified water, Milli-Q PLUS (Millipore, Molsheim, France) was used throughout the study.

3.2 Animals and Tumor Cell Line

Female Fischer F344 rats (purchased from Möllegard, Skensvend, Denmark) with a body mass of 170 to 230 grams were used for all experiments. The animals were anaesthetized with a mixture of Haldol (16.7%), Fentanyl (25%), and Midazolan (25%) in water, 0.4 ml/100 g.

The AY-27 TCC cell line was grown in RPMI-1640 medium containing 10% v/v FCS, L-glutamine (80 mg/l), penicillin (100 U/ml), streptomycin (100 U/ml), and fungizone (0.25 mg/ml). The cancer cells were subcultured approximately twice a week and grown at 37°C in a humidified atmosphere containing 5% CO_2. A preliminary study on AY-27 cell suspensions confirmed that they produced PpIX endogenously when exposed to HAL. The cells were seeded in medium at a density of 0.30 to 0.45×10^6 in 75 cm^2 cell culture dishes. After anaesthetization and catheterization, the rats received an acid/lye wash where the bladder was filled with HCl (0.3 ml, 0.1 M) for 15 seconds followed by NaOH neutralization (0.3 ml, 0.1 M, 15 s), then washed with PBS (3×0.6 ml) before AY-27 cell instillation (4×10^6/rat, 1 h) as described by Xiao et al.[25] To ensure homogenous distribution of the AY-27 cells inside the bladder, animals were rotated 90 deg every 15 minutes during the one-hour instillation period.

To determine the optimal point in time for PDT treatment of AY-27 urinary bladder TCC, a pilot study was performed with histological examinations on days 7, 14, and 28 after cell instillation. The results showed that the thickness of the bladder wall was best suited for PDT treatment at 14 days after instillation (data not shown).

Fig. 1 Photograph showing rat with fiberoptic probe for measurement (left), and rat with fiber applicator during light irradiation (right).

All animals showed normal behavior (eating, urinating, activity) during the test period of 21 days (28 days for pilot study).

3.3 PDT Treatment

On day 14 after AY-27 instillation, the animals were anaesthetized and catheterized with an 18 G catheter. The HAL solution (8 mM, 0.3 ml) was instilled in the bladder for 1 hour (animals were rotated 90 deg every 15 minutes). The light treatment was performed two hours after the end of HAL instillation, corresponding to the peak PpIX accumulation in the bladder tissue.[17]

The irradiation source consisted of an Argon-pumped (Innova 70, Coherent, Santa Clara, CA) dye laser (model 375, Spectra-Physics, Mountain View, CA) centered at 635 nm. Light was coupled into a 200-μm fiber applicator with an isotropic diffuser tip (PDT Systems, Santa Barbara, CA). The applicator was inserted through the 18-G catheter to illuminate the bladder, as shown in Fig. 1. The fluence rate was set to 20 mW/cm^2 for all animals (and corrected for the integrating sphere effect), then measured with an integrating sphere setup and a laser power meter (FieldMaxII-TOP, Molectron Corp., Sunnyvale, CA). Total light fluence was 20 J/cm^2. The bladders were filled with 0.3 ml saline to keep them distended during irradiation. All animals were kept anaesthetized and laid on a warming pad to maintain body temperature during the treatment period.

3.4 In Vivo Optical Spectroscopy

A forward-viewing fiber-optic probe was constructed to perform optical reflection and fluorescence spectroscopy of the rat bladders in vivo. The probe was constructed of three 200-μm optical fibers (FG-200-LCR/FT-200-EMT, ThorLabs, Newton, NJ), two illumination fibers, and one collection fiber. Fibers were mounted side by side in a triangle configuration, inserted in a 20-G needle as shown in Fig. 2, and cemented in place using UV-curing glass adhesive.

The length of the probe was constructed to be 1 mm longer than the 18-G catheter when fully inserted to ensure the same placement in the bladder and to standardize the measurements. However, the fiber placement and tip-to-wall distance was also dependent on the placement of the catheter and the geometry of the bladder. To ease handling, the fiber pigtails were placed inside protective jackets. The fibers were
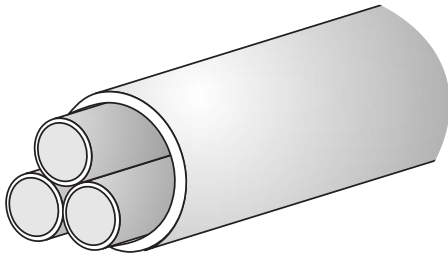
Fig. 2 Illustration of the forward-viewing fiberoptic probe, showing the three fibers protruding from the 20-G needle (not to scale).

Fig. 3 Representative fluorescence spectra from one animal in group VI showing both pre- (line) and post- (dash) laser treatment. The main PpIX fluorescence peak at 635 nm (vertical, dot) and the calculated baseline (dash-dot) for tissue autofluorescence are also shown.

terminated with SMA 905 connectors compatible with the measurement equipment. A preliminary study showed that if the probe was placed in direct contact with the bladder wall, the increased perfusion due to the mechanical irritation was visible in the reflectance spectra. However, light contact between the probe and tissue did not cause injury to the bladder lining. Erroneous measurements due to practical difficulties in some animals (bladder contraction, blood in bladder) were excluded.

The measurement setup consisted of a fiber-coupled spectrometer (SD2000, Ocean Optics, Duiven, The Netherlands), a white light source (LS-1, Ocean Optics), and a pulsed 337-nm (6 mW at 20 Hz) nitrogen laser (VSL-337ND, LaserScience Inc., Franklin, MA). Each one was coupled to a fiber on the probe. Before the reflectance measurements, the fiber probe was calibrated by inserting it into a small cylinder that was placed in close contact with a Spectralon reflectance standard (Ocean Optics). The cylinder ensured that no ambient light entered the detection system, and it kept a fixed distance between the probe tip and the standard. For fluorescence measurements, the fiber probe was positioned to maximize the fluorescence. The animals were covered by black felt to avoid interference from other light sources during measurements. Due to the small size of the urethra, the fiber probe had to be removed when the illumination fiber applicator was inserted, then reinserted after the laser treatment process. Hence, the first spectra recorded after laser treatment were collected within two minutes after illumination was terminated. The total detected fluorescence was the sum of the fluorescence contribution from PpIX and that of tissue autofluorescence. The PpIX fluorescence intensity (I_f) was calculated by normalizing spectra at 600 nm, and subsequently fitting a polynomial line between 600 and 660 nm as a baseline to represent tissue autofluorescence. The PpIX fluorescence was defined as the area above this baseline (see Fig. 3) in the interval between 615 and 655 nm (peak at 635 nm).

3.5 Oxygen Saturation

Hemoglobin is the most evident chromophore in perfused tissue. Various species of hemoglobin can be identified from the reflectance spectra, with oxygenated and deoxygenated hemoglobin being the two most common. Thus, knowing the absorbtion spectra of these chromophores makes it possible to calculate the oxygen saturation (OS) in the tissue,
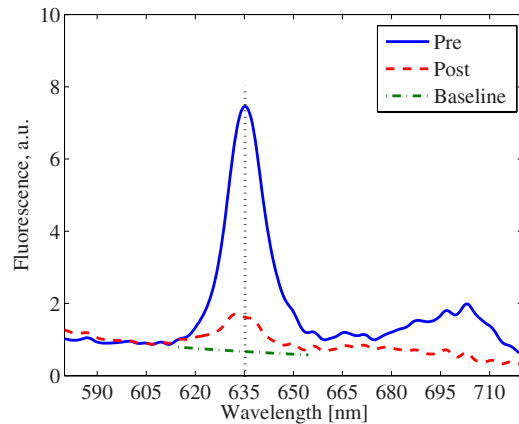
$$OS = \frac{HbO_2}{Hb_{\text{total}}} \cdot 100 \% \;, \tag{2}$$

where HbO_2 denotes the oxygenated hemoglobin, and Hb_{total} is the sum of all hemoglobin species in the blood. Due to the low collection efficiency of the fiber probe above 700 nm, and to the fact that oxygenated and deoxygenated hemoglobin have clear absorption peaks in the 520 to 590 nm region, this wavelength region was used to calculate the oxygen saturation. Measured spectra were simulated to yield the OS based on the hemoglobin absorption spectra.[26] Zijlstra et al. showed that rat hemoglobin had similar absorption spectra characteristics as human hemoglobin in this wavelength region.[27]

3.6 Treatment Protocol

The animals were divided into six groups, and each group received the treatment shown in Table 1. Three additional groups—no treatment $(n=3)$, only-HAL treatment $(n=3)$, and only light treatment $(n=2)$—were tested as controls.

Photosensitizer and light doses were kept equal for each animal: 8 mM of HAL combined with a light fluence of 20 J/cm^2, the amount shown to be optimal by Khatib et al. for treatment of superficial bladder cancer.[17]

Reflectance and fluorescence spectra were recorded for all groups shown in Table 1.

3.7 Statistical Analysis

Nonparametric methods were used to evaluate the fluorescence data due to a marked heterogeneity of variance between the different groups (the Levelene's test for equality of variance). Comparisons between groups of interest were carried out using Kruskal-Wallis (several groups) and Mann-Whitney U (two groups) tests, respectively. The changes in fluorescence level before and after laser treatment were evaluated using the Wilcoxon test. Parametric tests were used for normally distributed variables (OS values) using an unpaired t-test to compare between two groups, and paired sample t-tests to analyze for significant changes before and after laser treatment.

Table 1 Treatment protocol, where + denotes treatment received.

Group	No. of animals	Acid/lye wash	AY-27, cells	HAL 8 mM (1 h)	Laser 20 J/cm^2
I	6	+	+	−	−
II	6	+	+	+	−
III	8	+	+	−	+
IV	9	+	−	+	+
V	7	−	−	+	+
VI	18	+	+	+	+

Non-normally distributed variables were expressed as medians (25th and 75th percentiles) and normally distributed as means ± standard deviation (SD). Significance was defined as a p-value of less than 0.05 (two-tailed).

3.8 Histological Examination of Bladders

The animals were sacrificed 7 days after the PDT treatment. Each bladder was collected, instilled with buffered 4% formaldehyde for 24 h, and embedded in paraffin. Sections were cut through each tissue block at 4-μm thickness and stained with hematoxylin, eosin, and saferin (H.E.S) for histological examination. Sections were evaluated at low magnification ($10\times$) for the entire section, and at high magnification ($40\times$) for details of tissue destructions. The profile area (mm^2) of the tumor was measured by software (Nikon NIS-Elements Basic Research, Inter Instrument AS, Høvik, Norway). The evaluation was performed by a histologist blinded to the sample source.

4 Results

4.1 Fluorescence Spectra

Fluorescence measurements on group VI animals revealed that PpIX fluorescence decreased following laser treatment. A representative PpIX fluorescence spectrum from pre- and post-laser treatment for one group VI animal is shown in Fig.
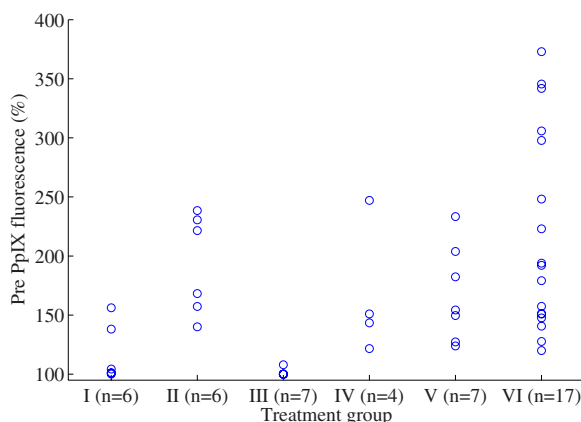
3. Pre-laser treatment PpIX fluorescence at 635 nm was observed in all groups as shown in Fig. 4 (differences in number of animals n from Table 1 are due to erroneous measurements that are excluded). PpIX fluorescence was also observed in HAL-treated animals despite the fact that they did not receive the AY-27 cells.

Figure 5 represents the pre-/post-PpIX fluorescence for groups III through VI. There was a significant decrease in PpIX fluorescence before and after laser treatment for group IV ($p=0.031$), group V ($p=0.008$), and group VI ($p<0.0005$). Fluorescence measurements 24 h after PDT in group VI animals did not show any sign of PpIX in the bladders.

4.2 Reflectance Spectra

Figure 6 shows reflectance spectra from groups V (HAL +light) and VI animals compared to a control animal (no treatment). The characteristic absorption peaks of oxyhemoglobin at 542 and 576 nm were clearly visible in the spectra recorded before the laser treatment. These peaks were not as evident in the spectrum recorded after laser treatment. Oxygen saturation of the bladder tissue was calculated from the reflectance spectra. No significant OS differences were observed in animals with only acid/lye washing before and after laser treatment. However, OS was slightly decreased in group
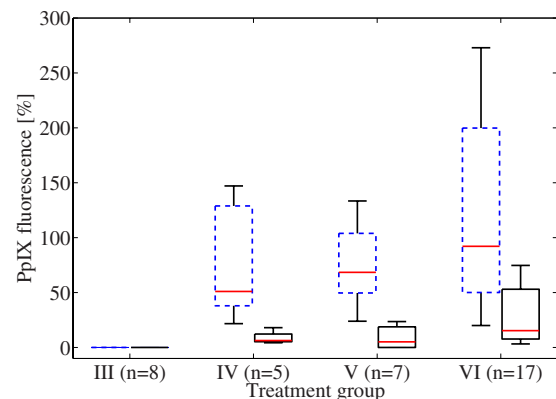

Fig. 4 Individual PpIX fluorescence values (%) before the laser treatment for groups I through VI.

Fig. 5 PpIX fluorescence (%) pre- (dashed) and post- (solid) laser treatment for groups III through VI. The boxplot shows the 25th, 50th (median), and 75th percentiles, and the vertical lines outside the box represent the largest and smallest values.
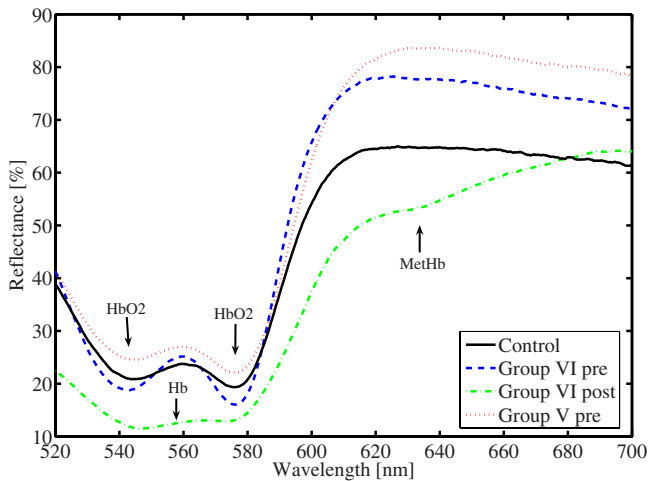
Fig. 6 Representative reflectance spectra of group V and VI animals.

Fig. 8 Representative micrographs showing transitional cell carcinoma in bladders 21 days after AY-27 cell implantation. (a) No PDT treatment; (b) 7 days after PDT treatment. (H.E.S. staining, photos taken at 10×.)

4.3 Macroscopic Examination

Macroscopic inspection of the cancerous bladders revealed that the cells had attached to the bladder wall and cancer had developed as islands of tumor cells inside the bladders. In a preliminary experiment, fluorescence measurements were performed on excised bladders that had cancer and received HAL instillation. PpIX fluorescence was not detected outside the cancerous islands (data not shown), confirming the high selectivity of HAL.

There were variations in the cancer masses that developed between different animals. The mean mass of cancerous bladders was 0.179 g, compared to 0.098 g for healthy bladders—an increase of 82.3%.

4.4 Histopathological Findings of the Urinary Bladder TCC

Tumors were found on the wall of the urinary bladder from all 6 rats in the AY-27 cell implantation group without PDT treatment [group I, Fig. 8(a)], and in 3 of 6 in the PDT-treated AY-27 cell implantation group [group VI, Fig. 8(b)]. The tumors were characterized by displaying high mitotic activity, high nuclear-to-cytoplasmic ratio, and marked nuclear pleomorphism (see Fig. 8). Most tumors (from both groups) appeared intraepithelial, and sometimes papillary tumors and/or lymphocytic and mononuclear cell infiltration around the tumor could be observed. The tissue outside of the tumor islands appeared to be normal in the untreated group. In the PDT-treated AY-27 implantation bladders, healed necrosed urothelium with complete regeneration of urothelium was observed in all rats. In the 3 of 6 bladders with remaining tumors, partial tumor damage was seen and the tumor area was severely reduced (see Table 2). No tumors were found in the control or PDT-treated normal rats (group V).

Differences in fluorescence intensity may partly explain the differences in tumor destruction of group VI. The 3 of 6 fully responsive animals in group VI corresponded to the animals that exhibited the largest prelaser-treatment PpIX fluorescence ($I_f = 206\%$, 242% and 273%, mean $240 \pm 33\%$). The other 3, not fully responsive animals did not exhibit as high of a pretreatment fluorescence ($I_f = 126\%$, 198% and 148%, mean $157 \pm 36\%$).

IV animals (acid/lye wash+HAL+light) after laser treatment, while it slightly increased after laser treatment for group V animals (HAL+light). None of the animals in these groups had carcinomas in the bladder. In contrast, all group-VI animals showed a clear decrease in tissue oxygenation following the laser treatment.

Figure 7 shows the oxygenation data calculated from the reflectance spectra. There was a significantly lower OS in animals implanted with AY-27 cells (groups I through III and VI) compared to animals without AY-27 cells (groups IV and V). Mean values were $64.5 \pm 13.4\%$ and $72.5 \pm 11.6\%$, respectively ($p = 0.047$). Oxygen saturation significantly decreased in group VI after laser treatment ($p = 0.0001$), but no significant difference was observed in the remaining groups. Methemoglobin (MetHb) was identified from the reflectance spectra of certain group VI animals. These animals also had the most marked deoxygenation of the bladder tissue after laser treatment.
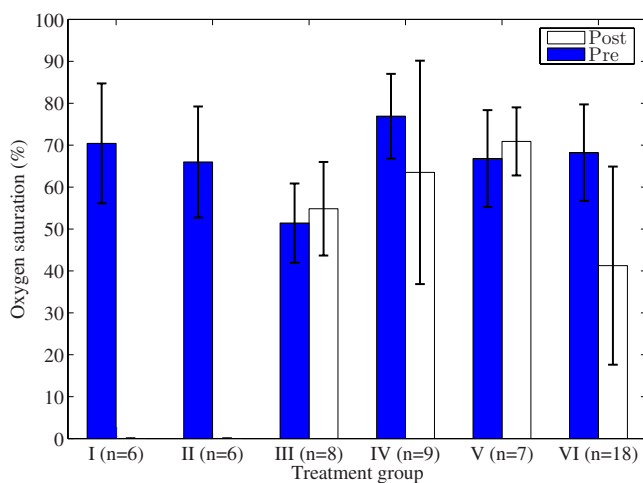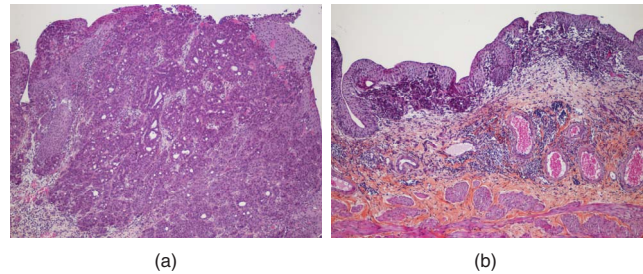

Fig. 7 Oxygen saturation (%) from pre-laser treatment (groups I and II), and from pre- and post-laser treatment (groups III through VI), presented as mean±SD.

4.5 Simulation Results

Simulated spectra suggested a large BV increase in the top layers of the model following HAL instillation, and this was

Table 2 TCC histological findings. Means±SD.

Group	Treatment	No. of animals	TCC	TCC area in specimen (mm^2)
—	Control	6	0/6	0
I	AY-27	6	6/6	1.016±0.207
V	PDT	6	0/6	0
VI	AY-27+PDT	6	3/6	0
			3/6	0.268±0.019

largely independent of the various layer thicknesses. A measured simulated spectra pair from a representative group VI animal is shown in Fig. 9. The dip in the reflection spectrum at 635 nm was only reproduced in the simulated spectrum by the introduction of MetHb.

5 Discussion and Conclusions

ALA ester derivatives have better diffusion properties than ALA alone as a result of their enhanced lipophilicity.[6,28] By applying HAL exogenously to cells, the esterase activity leads to the formation of 5-ALA, which will enter the heme-biosynthetic pathway. Gaullier et al. demonstrated (*in vitro*) that esterification of 5-ALA by long-chain aliphatic alcohols (C6 to C8) on the carbonyl group considerably increased the PpIX production.[6] An *in vivo* demonstration on a human bladder cancer confirmed these results.[11]

The results from the present study confirmed the endogenous production of PpIX in animals with bladder cancers instilled with HAL. However, porphyrins were detected not only in the group VI animals, but also in HAL-treated animals without cancer. A possible explanation for the observed PpIX
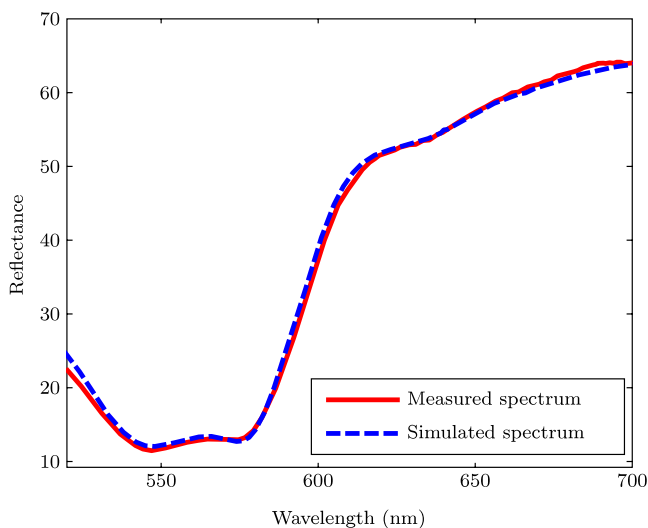

Fig. 9 Measurement of group VI animal (post-laser treatment) and corresponding simulated spectrum ($OS_{urothelium}=OS_{submucosa}=20\%$, $OS_{muscularis}=50\%$, $BV_{urothelium}=26\%$, $BV_{submucosa}=40\%$, $BV_{muscularis}=20\%$, MetHb=40%).

fluorescence in these animals without cancer may be due to the accumulation of HAL, and subsequently PpIX, in scars or small wounds in the bladder. These wounds may have been caused by the acid/lye wash or by the catheter/fiber probe. Preliminary measurements confirmed the high selectivity of HAL, because no PpIX fluorescence was detected outside the cancerous islands in the bladder. Very low PpIX fluorescence might be expected in normal bladder tissue, but this could not be detected with the present measurement system. In a previous work, Gederaas et al. measured the concentration of PpIX in ALA-stimulated WiDr cancer cells (*in vitro*) using high-pressure liquid chromatography (HPLC) techniques and found that the ALA-stimulated cells had about 25 times higher PpIX concentration than the control cancer cells.[29] Extracts of other cancer cell lines have also been analysed using fluorescence detection in solutions, but no PpIX fluorescence could be detected in control cells using a standard fluorescence spectrophotometer.[30]

As shown by others, photobleaching alone may not always be an appropriate measurement of singlet oxygen production and PDT dosimetry, and can even be unrelated.[31] Our results clearly show the photobleaching effects of PpIX fluorescence. Interestingly, from histology, the 3 of 6 fully responsive animals corresponded to the animals that exhibited the highest pretreatment PpIX fluorescence. The other 3 of 6 not fully responsive animals did not exhibit such a high pretreatment fluorescence, indicating that PpIX fluorescence may be used to predict the therapeutic effect of PDT. However, the number of animals histologically examined in these experiments was small, and certain physical aspects must also be accounted for. Due to the configuration of the measurement probe and the uncertain positioning of the probe inside the bladder, the recorded spectra may be influenced by both healthy and cancerous tissue. Hence, there was an element of uncertainty about whether the tumors inside the bladder were in the field of view of the probe. To some extent this was compensated for by moving the fiber probe inside the bladder during measurements, but this was a large limitation of the fiber probe and must be considered for future improvement of the probe.

Prior to laser irradiation, animals with carcinomas indicated a significantly lower oxygenation in the bladder compared to animals without carcinomas. This lower oxygenation was probably due to the microvasculature of the cancerous tissue, leading to a slightly hypoxic state. Following laser treatment, the observed OS decrease in group IV (acid/lye wash+HAL+light) might be due to the small levels of PpIX present. However, this does not explain the OS increase after laser treatment for group-V animals (HAL+light), which may be due to increased perfusion in the bladder wall as a result of an inflammatory response due to irritation of the bladder lining. The large OS decrease in group-VI animals following laser irradiation clearly showed that oxygen-consuming processes took place during treatment.

Solid tumors consist of regions with large numbers of hypoxic cells compared with the surrounding normal tissue. The hypoxic fraction varied between 1% and 79% of the total tumor volume in 42 experimental tumor models.[32] Tissue hypoxia is due to inadequate blood supply and is supposed to occur very early during tumor development.[33] The process of generating hypoxia may include various mechanisms of impaired intratumoral oxygen delivery (e.g., vascular abnormali-

ties, intratumoral pressure gradients, acute/chronic anemia) and consumption.[34]

Simulations of reflectance spectra suggest an increased blood perfusion to the bladder lining. This may indicate an increased blood perfusion close to the bladder lining, suggesting a reaction or inflammatory response to the drug. However, it was also possible that blood inside the bladder might have affected the measurements, since bloody urine was observed in some animals that most likely originated from small wounds due to the catheterization process. MetHb was found in only one batch of the group-VI animals (the experiment was performed three times with the same number of animals). These animals were also the most deoxygenated after laser treatment. This might be attributed to small variances in the anaesthetization of animals. MetHb is an indication of oxidative stress to the hemoglobin molecule, and can be formed by ultraviolet radiation (UV-B),[35] or thermally by heating or laser photothermolysis.[21] The production of MetHb also may be due to oxidative stress caused by reactive oxygen species.[36] Since MetHb was observed only in animals with the lowest oxygenation after treatment, it suggests that the formation of (measurable) MetHb requires the relatively large production of singlet oxygen, or it may result from an oxygen-independent process. Thus, MetHb formed during PDT might be used as an indirect measure of the photochemical processes. Whether the formation of MetHb may be used as a predictor for the treatment outcome still remains unresolved. Due to the partial overlap between MetHb and oxy/deoxyhemoglobin absorption spectra, the presence of MetHb (if not accounted for) may affect OS calculations.

During the laser treatment of the group-VI animals, saline keeping the bladder distended slowly leaked out. This suggests that HAL may have penetrated into the muscle layer of the bladder, causing bladder contractions as a response to the treatment. In one animal it was even impossible to refill the bladder with saline after the laser treatment, which might be partly due to diminishing anesthetics. A smaller bladder volume alters the light dosimetry parameters, because the decreased area leads to a higher light fluence rate, causing increased irradiation of the tissue.

Photobleaching of PpIX fluorescence and a local increase of oxygen consumption in the tumors demonstrate the production of ROS during PDT. There were traces of PpIX after laser treatment, so there was still a potential for more PDT-induced damage of the tissue. However, the remaining PpIX might be attributed to an insufficient light fluence or a reduced oxygen availability in the tissue, thus limiting the efficacy of the treatment.

Histology has shown that a fluence of 20 J/cm^2 (20 mW/cm^2) combined with 8 mM of HAL (1 h) is an appropriate dose for HAL-based PDT treatment of rat TCC.. However, optimization is required to achieve better treatment results. Optical spectroscopy can be a useful tool in tailoring individual treatment parameters for each patient.

Instillation of AY-27 cells through a catheter following an acid/lye wash has proven to be a very suitable method for bladder cancer studies. This study does not provide information on the penetration depth of HAL through the plasma membrane (passive diffusion), but histological data on rat bladders indicate that the tumor penetration level at 14 days from initial instillation should be ideal for such experiments.

Optical spectroscopy can provide important information for PDT treatment, but more research is necessary to identify the most important factors for PDT optimization of bladder cancers.

References

1. D. M. Parkin, F. Bray, J. Ferlay, and P. Pisani, "Estimating the world cancer burden: Globocan 2000," *Int. J. Cancer* **94**, 153–156 (2001).
2. U. O. Nseyo, J. DeHaven, T. J. Dougherty, W. R. Potter, D. L. Merrill, S. L. Lundahl, and D. L. Lamm, "Photodynamic therapy (PDT) in the treatment of patients with resistant superficial bladder cancer: a long-term experience," *J. Clin. Laser Med. Surg.* **16**(1), 61–68 (1998).
3. K. Plaetzer, T. Kiesslich, T. Verwanger, and B. Krammer, "The modes of cell death induced by PDT: An overview," *Med. Laser Appl.* **18**, 7–19 (2003).
4. Q. Peng, T. Warloe, K. Berg, J. Moan, M. Kongshaug, K.-E. Giercksky, and J. M. Nesland, "5-aminolevulinic acid based photodynamic therapy: Principles and experimental research," *Photochem. Photobiol.* **65**(22), 235–251 (1997).
5. N. I. Berlin, A. Neuberger, and J. J. Scott, "The metabolism of δ-aminolevulinc acid," *Biochem. J.* **64**, 80–90 (1956).
6. J. M. Gaullier, K. Berg, Q. Peng, H. Anholt, P. K. Selbo, L. W. Ma, and J. Moan, "Use of 5-aminolevulinic acid esters to improve photodynamic therapy on cells in culture," *Cancer Res.* **57**, 1481–1486 (1997).
7. O. A. Gederaas, A. Holroyd, S. B. Brown, D. Vernon, J. Moan, and K. Berg, "5-aminolevulinic acid methyl ester transport on amino acid carriers in a human colon adenocarcinoma cell line," *Photochem. Photobiol.* **73**(2), 164–169 (2001).
8. Z. Luksiene, I. Eggen, J. Moan, J. M. Nesland, and Q. Peng, "Evaluation of protoporphyrin IX production, phototoxicity and cell death pathway induced by hexylester of 5-aminolevulinic acid in Reh and HPB-ALL cells," *Cancer Lett.* **169**, 33–39 (2001).
9. M. Kriegmair, R. Baumgartner, R. Knuechel, P. Steinbach, A. Ehsan, W. Lumper, F. Hofstädter, and A. Hofstetter, "Fluorescence photodetection of neoplastic urothelial lesions following intravesical instillation of 5-aminolevulinic acid.," *Urology* **44**(6), 836–841 (1994).
10. P. Jichlinski, M. Forrer, J. Mizeret, T. Glanzmann, D. Braichotte, G. Wagnieres, G. Zimmer, L. Guillou, F. Schmidlin, P. Graber, H. van den Bergh, and H. Leisinger, "Clinical evaluation of a method for detecting superficial surgical transitional cell carcinoma of the bladder by light-induced fluorescence of protoporphyrin IX following the topical application of 5-aminolevulinic acid: preliminary results," *Lasers Surg. Med.* **20**(4), 402–408 (1997).
11. N. Lange, P. Jichlinski, M. Zellweger, M. Forrer, A. Marti, L. Guillou, P. Kucera, G. Wagnieres, and H. van den Bergh, "Photodetection of early human bladder cancer based on the fluorescence of 5-aminolaevulinic acid hexylester-induced protoporphyrin IX: a pilot study," *Br. J. Cancer* **80**, 185–193 (1999).
12. Y. Fradet, H. B. Grossman, L. Gomella, S. Lerner, M. Cookson, D. Albala, and M. J. Droller, "A comparison of hexaminolevulinate fluorescence cystoscopy and white light cystoscopy for the detection of carcinoma in situ in patients with bladder cancer: A phase iii, multicenter study," *J. Urol. (Baltimore)* **178**, 68–73 (2007).
13. J. F. Bisson, M. Christophe, J. J. Padilla-Ybarra, D. Notter, C. Vigneron, and F. Guillemin, "Determination of the maximal tumor:normal bladder ratio after i.p. or bladder administration of 5-aminolevulinic acid in fischer 344 rats by fluorescence spectroscopy in situ," *Anti-Cancer Drugs* **13**, 851–857 (2002).
14. J. Moan, G. Streckyte, S. Bagdonas, Ø. Bech, and K. Berg, "Photobelaching of protoporphyrin IX in cells incubated with

5-aminolevulinic acid," *Int. J. Cancer* **70**, 90–97 (1997).

15. H.-W. Wang, M. E. Putt, M. J. Emanuele, D. B. Shin, E. Glatstein, A. G. Yodh, and T. M. Busch, "Treatment-induced changes in tumor oxygenation predict photodynamic therapy outcome," *Cancer Res.* **64**, 7553–7561 (2004).

16. Z. Xiao, K. Brown, J. Tulip, and R. B. Moore, "Whole bladder photodynamic therapy for orthotopic superficial bladder cancer in rats: a study of intravenous and intravesical administration of photosensitizers," *J. Urol. (Baltimore)* **169**, 352–356 (2003).

17. S. E. Khatib, J. Didelon, A. Leroux, L. Bezdetnaya, D. Notter, and M. D'Hallewin, "Kinetics, biodistribution and therapeutic efficacy of hexylester 5-aminolevulinate induced photodynamic therapy in an orthotopic rat bladder tumor model," *J. Urol. (Baltimore)* **172**, 2013–2017 (2004).

18. J. P. A. Marijnissen, W. M. Star, H. J. A. in't Zandt, M. A. D'Hallewin, and L. Baert, "*In situ* light dosimetry during whole bladder wall photodynamic therapy: clinical results and experimental verification," *Phys. Med. Biol.* **38**, 567–582 (1993).

19. B. J. Tromberg, L. O. Svaasand, M. K. Fehrt, S. J. Madsen, P. Wyss, B. Sansone, and Y. Tadir, "A mathematical model for light dosimetry in photodynamic destruction of human endometrium," *Phys. Med. Biol.* **41**, 223–237 (1996).

20. H. H. Pennes, "Analysis of tissue and arterial blood temperatures in the resting human forearm," *J. Appl. Physiol.* **1**(2), 93–122 (1948).

21. L. L. Randeberg, J. H. Bonesrønning, M. Dalaker, J. S. Nelson, and L. O. Svaasand, "Methemoglobin formation during laser induced photothermolysis of vascular skin lesions," *Lasers Surg. Med.* **34**(5), 414–419 (2004).

22. A. Huygens, A. R. Kamuhabwa, B. V. Cleynenbreugel, H. V. Poppel, T. Roskams, and P. A. M. D. Witte, "*In vivo* accumulation of different hypericin ion pairs in the urothelium of the rat bladder," *BJU Int.* **95**(3), 436–441 (2005).

23. W. F. Cheong, S. A. Prahl, and A. J. Welch, "A review of the optical properties of biological tissues," *IEEE J. Quantum Electron.* **26**(12), 2166–2185 (1990).

24. G. A. Boorman, J. R. Gauger, T. R. Johnson, M. J. Tomlinson, J. Findlay, G. S. Travlos, and D. L. McCormick, "Eight-week toxicity study of 60 hz magnetic fields in f344 rats and b6c3f1 mice," *Fundam. Appl. Toxicol.* **35**, 55–63 (1997).

25. Z. Xiao, T. J. McCallum, K. M. Brown, G. G. Miller, S. B. Halls, I. Parney, and R. B. Moore, "Characterization of a novel transplantable orthotopic rat bladder transplantable orthotopic rate bladder transitional cell tumour model," *Br. J. Cancer* **81**(4), 638–646 (1999).

26. S. Prahl, "Optical absorption of hemoglobin," Oregon Medical Laser Center, http://omlc.ogi.edu/spectra/hemoglobin.

27. W. G. Ziljstra, A. Buursma, H. E. Falke, and J. F. Catsburg, "Spectrophotometry of hemoglobin: absorption spectra of rat oxyhemoglobin, deoxyhemoglobin, carboxyhemoglobin, and methemoglobin," *Comp. Biochem. Physiol., Part B: Biochem. Mol. Biol.* **107**(1), 161–166 (1994).

28. Q. Peng, T. Warloe, K. Berg, J. Moan, M. Kongshaug, K.-E. Giercksky, and J. M. Nesland, "5-aminolevulinic acid based photodynamic therapy," *Cancer* **79**, 2282–2308 (1997).

29. O. A. Gederaas, K. Berg, and I. Romslo, "A comparative study of normal and reverse phase high pressure liquid chromatography for analysis of porphyrins accumulated after 5-aminolevulinic acid treatment of colon adenocarcinoma cells," *Cancer Lett.* **150**, 205–213 (2000).

30. O. A. Gederaas, S. A. Schønberg, S. Ramstad, K. Berg, A. Johnsson, and H. E. Krokan, "Cell specific effects of polyunsaturated fatty acids on 5-aminolevulinic acid based photosensitization," *Photochem. Photobiol. Sci.* **4**, 383–389 (2005).

31. S. Iinuma, K. T. Schomacker, G. Wagniers, M. Rajadhyaksha, M. Bamberg, T. Momma, and T. Hasan, "*In vivo* fluence rate and fractionation effects on tumor response and photobleaching: Photodynamic therapy with two photosensitizers in an orthotopic rat tumor model," *Cancer Res.* **59**, 6164–6170 (1999).

32. J. E. Moulder and S. Rockwell, "Hypoxic fractions of solid tumors: experimental techniques, methods of analysis, and a survey of existing data," *Int. J. Radiat. Oncol., Biol., Phys.* **10**, 695–712 (1984).

33. M. Kunz and S. M. Ibrahim, "Molecular responses to hypoxia in tumor cells," *Mol. Canc.* **2**, 23 (2003).

34. L. B. Harrison, M. Chadha, R. J. Hill, K. Hu, and D. Shasha, "Impact of tumor hypoxia and anemia on radiation therapy outcomes," *Oncologist* **7**(6), 492–508 (2002).

35. L. S. Demma and J. M. Salhany, "Direct generation of superoxide anions by flash photolysis of human oxyhemoglobin," *J. Biol. Chem.* **252**(4), 1226–1230 (1977).

36. A. Mal, A. Nandi, and I. B. Chatterjee, "Haemoglobin: A scavenger of superoxide radical," *J. Biosci.* **16**(1 & 2), 45–53 (1991).